Determination of $\eta \to \pi^+\pi^-\pi^0$ Dalitz Plot slopes and asymmetries with the KLOE detector.

The KLOE Collaboration

F. Ambrosino [d,1], A. Antonelli [a], M. Antonelli [a], F. Archilli [a], C. Bacci [i], P. Beltrame [b], G. Bencivenni [a], S. Bertolucci [a], C. Bini [g], C. Bloise [a], S. Bocchetta [i], V. Bocci [g], F. Bossi [a], P. Branchini [i], R. Caloi [g], P. Campana [a], G. Capon [a], T. Capussela [a,1], F. Ceradini [i], S. Chi [a], G. Chiefari [d], P. Ciambrone [a], E. De Lucia [a], A. De Santis [g], P. De Simone [a], G. De Zorzi [g], A. Denig [b], A. Di Domenico [g], C. Di Donato [d], S. Di Falco [e], B. Di Micco [i], A. Doria [d], M. Dreucci [a], G. Felici [a], A. Ferrari [a], M. L. Ferrer [a], G. Finocchiaro [a], S. Fiore [g], C. Forti [a], P. Franzini [g], C. Gatti [a], P. Gauzzi [g], S. Giovannella [a], E. Gorini [c], E. Graziani [i], M. Incagli [e], W. Kluge [b], V. Kulikov [ℓ], F. Lacava [g], G. Lanfranchi [a], J. Lee-Franzini [a,j], D. Leone [b], M. Martini [a], P. Massarotti [d], W. Mei [a], S. Meola [d], S. Miscetti [a], M. Moulson [a], S. Müller [a], F. Murtas [a], M. Napolitano [d], F. Nguyen [i], M. Palutan [a], E. Pasqualucci [g], A. Passeri [i], V. Patera [a,f], F. Perfetto [d,1], M. Primavera [c], P. Santangelo [a], G. Saracino [d], B. Sciascia [a], A. Sciubba [a,f], F. Scuri [e], I. Sfiligoi [a], T. Spadaro [a], M. Testa [g], L. Tortora [i], P. Valente [g], B. Valeriani [b], G. Venanzoni [a], R.Versaci [a], G. Xu [a,k]

[a] *Laboratori Nazionali di Frascati dell'INFN, Frascati, Italy.*

[b] *Institut für Experimentelle Kernphysik, Universität Karlsruhe, Germany.*

[c] *Dipartimento di Fisica dell'Università e Sezione INFN, Lecce, Italy.*

[d] *Dipartimento di Scienze Fisiche dell'Università "Federico II" e Sezione INFN, Napoli, Italy*

[e] *Dipartimento di Fisica dell'Università e Sezione INFN, Pisa, Italy.*

[f] *Dipartimento di Energetica dell'Università "La Sapienza", Roma, Italy.*

[g] *Dipartimento di Fisica dell'Università "La Sapienza" e Sezione INFN, Roma, Italy.*

[h] *Dipartimento di Fisica dell'Università "Tor Vergata" e Sezione INFN, Roma, Italy.*

[i] *Dipartimento di Fisica dell'Università "Roma Tre" e Sezione INFN, Roma, Italy.*

[j] *Physics Department, State University of New York at Stony Brook, USA.*

[k] *Permanent address: Institute of High Energy Physics of Academica Sinica, Beijing, China.*

[ℓ] *Permanent address: Institute for Theoretical and Experimental Physics, Moscow, Russia.*

Abstract

We have studied, with the KLOE detector at the DAΦNE Φ-Factory, the dynamics of the decay $\eta \to \pi^+ \pi^- \pi^0$ using data from the radiative $\Phi \to \eta\gamma$ decay for an integrated luminosity $L = 450\,\text{pb}^{-1}$. From a fit to the Dalitz plot density distribution we obtain a precise measurement of the slope parameters. This should allow to improve the knowledge of the decay amplitude which is sensitive to the u-d quark mass difference. We also present new best results on the C-violating asymmetries in the $\eta \to \pi^+ \pi^- \pi^0$ decay.

[1] Corresponding authors.

E-mail address: Fabio.Ambrosino@na.infn.it (F. Ambrosino)

Tiziana.Capussela@lnf.infn.it (T. Capussela)

Francesco.Perfetto@na.infn.it (F. Perfetto).

1 Introduction

The decay of the isoscalar η into three pions occurs through isospin violation and thus is sensitive to the up-down quark mass difference. The electromagnetic corrections to the decay are small (Sutherland's theorem [1]) and do not affect significantly the rate or the Dalitz plot density [2].
Neglecting electromagnetic corrections, the decay amplitude is given by [3]:

$$A(s,t,u) = \frac{1}{Q^2}\frac{m_K^2}{m_\pi^2}\left(m_\pi^2 - m_K^2\right)\frac{M(s,t,u)}{3\sqrt{3}F_\pi^2} \tag{1}$$

where

$$Q^2 \equiv \frac{m_s^2 - \hat{m}^2}{m_d^2 - m_u^2} \tag{2}$$

is a combination of quark masses and $\hat{m} = \frac{1}{2}(m_u + m_d)$ is the average u, d quark mass, $F_\pi = 92.4$ MeV is the pion decay constant and $M(s,t,u)$ contains all the dependence of the amplitude on the Mandelstam invariants. Since the decay rate is proportional to Q^{-4},

$$\Gamma\left(\eta \to \pi^+\pi^-\pi^0\right) \propto |A|^2 \propto Q^{-4} \tag{3}$$

the transition $\eta \to 3\pi$ is, in principle, a very sensitive probe to determine Q. A theoretical estimate of Q is obtained from the Dashen theorem [2] [4] according to which

$$Q^2_{Dashen} = \frac{m_K^2}{m_\pi^2}\frac{m_K^2 - m_\pi^2}{m_{K^0}^2 - m_{K^+}^2 + m_{\pi^+}^2 - m_{\pi^0}^2} = (24.1)^2. \tag{4}$$

Of course, in order to extract the quark mass ratio from the decay width, one needs an accurate description of $M(s,t,u)$.
At lowest order

$$M(s,t,u) = \frac{3s - 4m_\pi^2}{m_\eta^2 - m_\pi^2}. \tag{5}$$

a well known result, based on Current Algebra. Integrating eq.(5) over the phase space and using the quark masses as estimated by Leutwyler [5] one obtains the following prediction for the decay rate [3] :

$$\Gamma^{theo}\left(\eta \to \pi^+\pi^-\pi^0\right) = 66 \text{ eV} \tag{6}$$

which strongly disagrees with the experimental value [6]:

$$\Gamma^{exp}\left(\eta \to \pi^+\pi^-\pi^0\right) = 295 \pm 16 \text{ eV}. \tag{7}$$

[2] The Dashen theorem states that in the chiral limit the charged kaon and pion electromagnetic mass shifts are the same: $\left(m_{\pi^+}^2 - m_{\pi^0}^2\right)_{em} = \left(m_{K_+}^2 - m_{K^0}^2\right)_{em}$

A one-loop calculation within conventional chiral perturbation theory (χPT) [7], improves considerably the prediction:

$$\Gamma^{theo}\left(\eta \to \pi^+\pi^-\pi^0\right) \simeq 167 \pm 50 \text{ eV}. \tag{8}$$

but is still far from the experimental value.
Higher order corrections discussed in the literature [3] contribute to increase the theoretical prediction, but cannot fully account for the discrepancy with the data. More recently a good agreement has been found combining the effective chiral Lagrangian with a non perturbative scheme based on coupled channels and Bethe Salpeter equation [8].
A significant violation of the Dashen theorem could in principle account for the discrepancy; however it should be claimed only after demonstrating agreement between theory and experiment on the $M(s,t,u)$ amplitude behaviour over phase space.
The above discussion therefore motivates a precise measurement of the $\eta \to 3\pi$ dynamics through the study of the Dalitz plot.
The Dalitz plot of the $\eta \to \pi^+\pi^-\pi^0$ decay is described by two kinematic variables. By convention these are defined in terms of the kinetic energies of the pions T_+, T_- and T_0 in the η rest frame:

$$X = \sqrt{3}\frac{T_+ - T_-}{Q_\eta} = \frac{\sqrt{3}}{2M_\eta Q_\eta}\,(u-t)\,,$$
$$Y = \frac{3T_0}{Q_\eta} - 1 = \frac{3}{2M_\eta Q_\eta}\left[((m_\eta - m_{\pi^0})^2 - s\right] - 1,$$
$$Q_\eta = m_\eta - 2m_{\pi^+} - m_{\pi^0}\,,$$

where X and Y respectively vary in the range $[-1,1]$ and $[-1,0.895]$.
The decay amplitude is then expanded around the center of the Dalitz plot (X=Y=0) in powers of X and Y as:

$$|A(X,Y)|^2 \simeq 1 + aY + bY^2 + cX + dX^2 + eXY + ... \tag{9}$$

and the parameters $(a,b,c,d,e,...\ )$ of the expansion are fitted to the experimental data. Any odd power of X contributing to $|A(X,Y)|^2$ would imply violation of Charge Conjugation.

2 The KLOE detector

Data were collected with the KLOE detector at DAΦNE [9], the Frascati e^+e^- collider, which operates at a center of mass energy $\sqrt{s} = M_\Phi$ $\sim$1020 MeV/c^2. The electron and positron beams collide with a crossing angle of $\pi - 25$ mrad, resulting in a small momentum ($p_\phi \sim 13$ MeV/c in the horizontal plane) of the produced ϕ mesons.

The KLOE detector consists of a large cylindrical drift chamber (DC), surrounded by a fine sampling lead-scintillating fibers electromagnetic calorimeter (EMC) inserted in a 0.52 T magnetic field..

The DC [10], 4 m diameter and 3.3 m long, has full stereo geometry and operates with a gas mixture of 90% Helium and 10% Isobutane. Momentum resolution is $\frac{\sigma_{p_T}}{p_T} \leq 0.4\%$. Position resolution in $r-\phi$ is 150 μm and $\sigma_z \sim 2$ mm. Charged tracks vertices are reconstructed with an accuracy of $\sim$3 mm.

The EMC [11] is divided into a barrel and two endcaps, for a total of 88 modules, and covers 98% of the solid angle. Arrival times of particles and space positions of the energy deposits are obtained from the signals collected at the two ends of the calorimeter modules, with a granularity of $\sim$(4.4 x 4.4) cm^2, for a total of 2240 cells arranged in five layers. Cells close in time and space are grouped into a calorimeter cluster. The cluster energy E is the sum of the cell energies, while the cluster time T and its position R are energy weighted averages. The respective resolutions are $\sigma_E/E = 5.7\%/\sqrt{E(GeV)}$ and $\sigma_T = 57$ ps$/\sqrt{E(GeV)} \oplus 100$ ps.

The KLOE trigger [12] is based on the coincidence of at least two energy deposits in the EMC, above a threshold that ranges between 50 and 150 MeV. In order to reduce the trigger rate due to cosmic rays crossing the detector, events with a large energy release in the outermost calorimeter planes are vetoed.

3 Signal selection and efficiency

At KLOE η mesons are produced in the process $\phi \to \eta\gamma$, so to study the dynamics of $\eta \to \pi^+\pi^-\pi^0$ the final state $\pi^+\pi^-\gamma\gamma\gamma$ is used to which corresponds a BR value of:

$$BR_{TOT} = BR\left(\phi \to \eta\gamma\right) \times BR\left(\eta \to \pi^+\pi^-\pi^0\right) \times BR\left(\pi^0 \to \gamma\gamma\right) = 2.9 \cdot 10^{-3}.$$

There is no combinatorial problem in the photon pairing because this decay chain is characterised by an energetic monochromatic recoil photon, with $E_{\gamma_{rec}} \sim 363$ MeV, quite well separated from the softer photons from π^0 decay.

In the data analysis a photon is defined as a cluster in the EmC with no associated track detected in the Drift Chamber (DC) and with $|(T - \frac{R}{c})| < 5\sigma_T$; where T is the arrival time on the EmC, R is the distance of the cluster from the vertex, c is the light speed and σ_T is the time resolution.

The events selection is performed through the following steps:

(1) Events are selected starting from a very loose offline preselection consisting of a machine background filter (FILFO) and an event selection procedure (EVCL) that assigns events into categories [13].

(2) One charged vertex is required inside the cylindrical region $r < 4$ cm, $|z| < 8$ cm and 3 photons with $21^\circ < \theta_\gamma < 159^\circ$ and $E_\gamma > 10$ MeV. The probability of a photon to fragment in more than a cluster (splitting) is reduced by requiring the opening angle between any pair of photons to be $> 18^\circ$.

(3) $\sum E_\gamma < 800\,\text{MeV}$.

(4) A constrained kinematic fit is performed imposing 4-momentum conservation and $t = \frac{R}{c}$ for each photon, without imposing mass constraint both on η and π^0.

A cut on the χ^2 probability is done, $\text{P}(\chi^2) > 1\%$.

This fit improves significantly the resolution on photon energies. The χ^2 distribution of the fit shows a satisfactory Data-MC agreement as shown in fig.1:

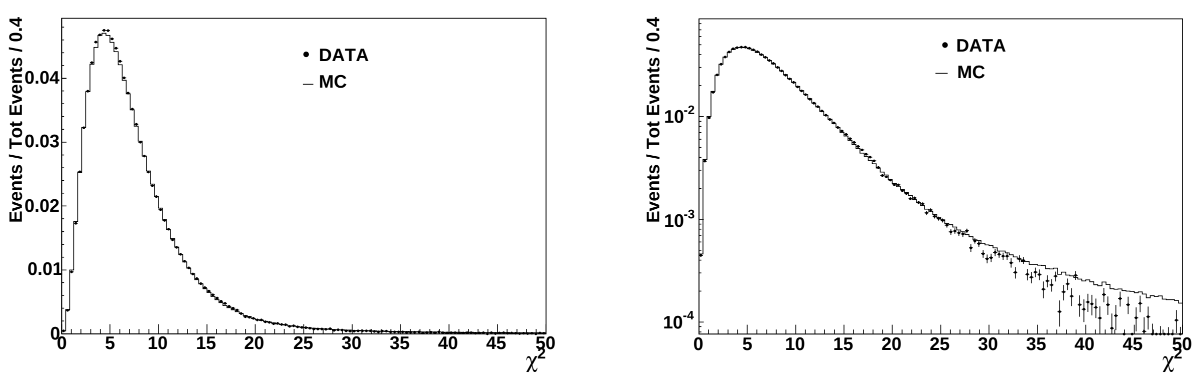

Fig. 1. χ^2 distribution for the kinematic fit. Left: linear scale; Right: log scale.

(5) Finally we require:

- $320\,\text{MeV} < E_{\gamma rec} < 400\,\text{MeV}$ for the recoil photon (to reduce residual background from $\phi \to K_S\,K_L$ events).

- E_{π^+}+E_{π^-} < 550 MeV (to reduce residual background from $\phi \to \pi^+\pi^-\pi^0$events).
- the invariant mass of the two softest photons: $M_{\gamma\gamma} \in [110, 160]$ MeV (to reduce residual background from $\eta \to \pi^+\pi^-\pi^0$ decays with $\pi^0 \to e^+e^-\gamma$ and from $\phi \to \eta\gamma$ events with $\eta \to \pi^+\pi^-\gamma$).

The selection efficiency is determined by using the KLOE MonteCarlo (MC) simulation program [13] and checked on data by means of control samples. In particular:

- The trigger efficiency evaluated by MonteCarlo is 99.9%, and we have excellent Data-MC agreement for the trigger sectors multiplicities.
- The effect of the event classification procedure (EVCL) and machine background filter is evaluated using a downscaled sample of non filtered data to which we apply much less stringent cuts in order to have a "minimum bias" selection. On signal events the efficiency of the minimum bias selection is 99.88%.

  We have found that the EVCL procedure introduces a signal loss of $\sim 1.5\%$, expected also from Monte Carlo estimates. The corresponding bias on the Dalitz plot parameters measurement has been evaluated and included in the systematic error. No bias is introduced by the FILFO procedure.

- The tracking and vertex efficiencies have been estimated from the Data-MC ratio observed for a control sample of $\phi \to \pi^+\pi^-\pi^0$ events selected to have charged-pion momenta in the same range as those from the $\eta \to \pi^+\pi^-\pi^0$ decay [14]:

$$\frac{(\varepsilon^2_{TRK}\varepsilon_{VTX})_{Data}}{(\varepsilon^2_{TRK}\varepsilon_{VTX})_{MC}} = 0.974 \pm 0.006. \tag{10}$$

  The Data-MC ratio of efficiencies is flat all over the momentum spectrum, thus introducing no bias in the Dalitz plot fit. We recall that all the variables used in the fit are evaluated in the η rest frame, which is boosted with respect to the laboratory by about 363 MeV/c momentum. Therefore to each momentum bin in the lab frame corresponds a much wider momentum interval in the η cms: any Data-MC discrepancy in the lab frame is further diluted by this effect.

- A correction to the detection efficiency for low energy photons has been obtained by comparing the photon energy spectrum of a data subsample to the expected MC spectrum; the average correction factor is 0.964.

The overall selection efficiency, taking into account all the Data-MC corrections is found to be $\varepsilon = (33.4 \pm 0.2)\%$. The expected background contamination, obtained from MC simulation is as low as 0.3%.

After the background subtraction the observed number of events is:

$$N_{obs} = 1.337 \pm 0.001 \quad \text{Mevts.}$$

The distribution of the data in the Dalitz plot is shown in fig.2.

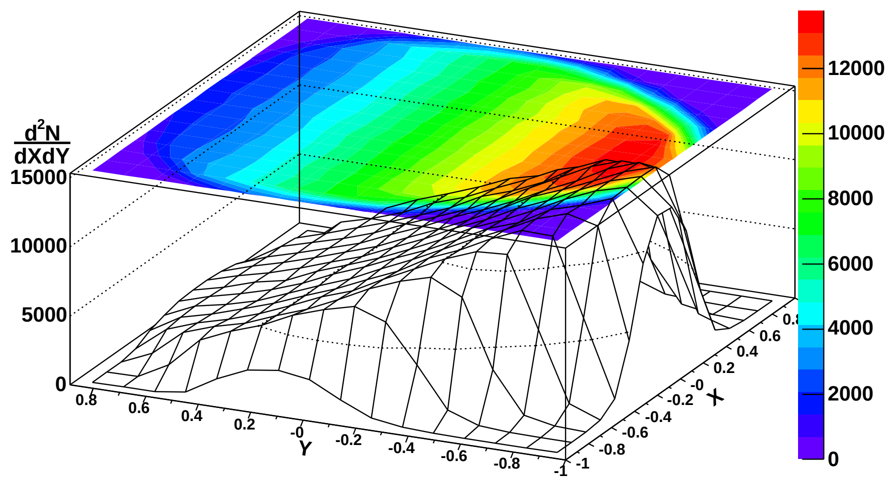

Fig. 2. Dalitz-plot distribution for the whole data sample. The plot contains 1.34 millions of events in 256 bins.

The signal selection efficiency $\varepsilon(X, Y)$ as function of Dalitz plot point is obtained by MC, for each (X, Y) bin, as the ratio:

$$\varepsilon(X, Y) = \frac{N_{rec}(X, Y)}{N_{gen}(X, Y)} \tag{11}$$

where $N_{rec}(X, Y)$ and $N_{gen}(X, Y)$ are respectively the reconstructed and generated Dalitz distributions. This definition of efficiency takes into account the smearing effects due to the finite resolution in X, Y. This approach is equivalent to the use of the complete four-dimensional smearing matrix as long as the MC correctly reproduces the Dalitz plot shape. To this aim we have used a data subsample to obtain a first estimate of the Dalitz plot parameters which we have used in final MC.
The efficiency $\varepsilon(X, Y)$ has a smooth behaviour all over the Dalitz plot. The projections of $\varepsilon(X, Y)$ on the X and Y axis are plotted in fig.3. While the efficiency appears to be rather flat on X (and symmetric in X as expected), it decreases in an

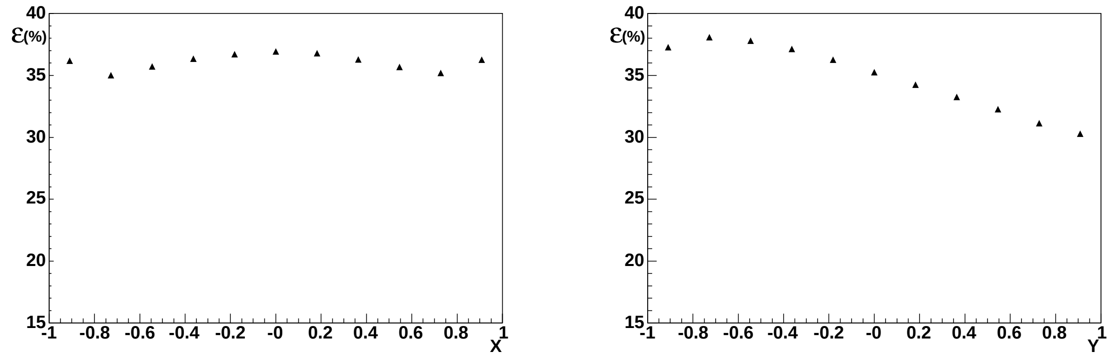

Fig. 3. Left: Efficiency versus X. Right: Efficiency versus Y.

approximately linear way with Y. In fact a large value for Y means a low-momentum $\pi^{\pm}$ in the decay to which corresponds a lower tracking/vertexing efficiency.
The expected resolutions on the Dalitz variables (X, Y) are shown in fig.4. The core resolution on X is about 0.02, due to our excellent momentum resolution for charged tracks. The Y variable, which is proportional to the π^0 kinetic energy, is evaluated [15] as the average between the "direct" determination obtained from the energy and direction of the two clusters associated to the $\pi^0 \to \gamma\gamma$ decay and the "indirect" determination : $T_0 = M_\eta - (E_{\pi^+} + E_{\pi^-}) - M_{\pi^0}$. This leads to a core resolution on Y of about 0.02.

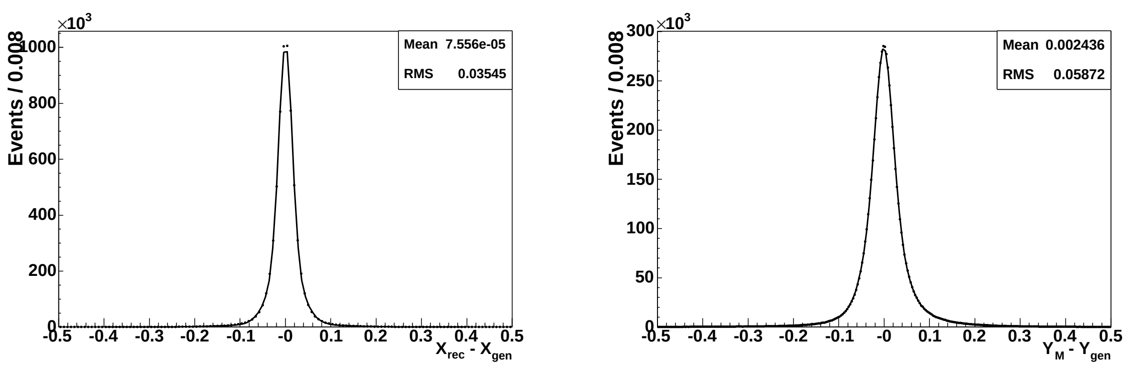

Fig. 4. Resolutions on X (left) and Y (right) according to MC. The curves are fitted to a sum of four gaussians.

4 Fit of Dalitz plot

The fit to the Dalitz plot is done using a least squares approach. Let $|A(X,Y)|^2$ be the theoretical squared amplitude:

$$|A(X,Y)|^2 = N(1 + aY + bY^2 + cX + dX^2 + eXY + ...). \tag{12}$$

with N being a normalization constant.
Then the χ^2 is defined as:

$$\chi^2 = \sum_i \sum_j \left(\frac{N_{ij} - \varepsilon_{ij} \int_{x_i}^{x_i+\Delta x} \int_{y_j}^{y_j+\Delta y} |A(X,Y)|^2 dPh(X,Y)}{\sigma_{ij}} \right)^2 \tag{13}$$

where dPh(X,Y) is the phase space element and for each bin (i,j):

- N_{ij} is the number of observed events in the bin,
- ε_{ij} is the signal selection efficiency,
- $(x_i, x_i + \Delta x)$ and $(y_j, y_j + \Delta y)$ are the bin boundaries,
- $\sigma_{ij} = \frac{N_{ij}}{\varepsilon_{ij}} \sqrt{\frac{1}{N_{ij}} + \left(\frac{(\delta\varepsilon)_{ij}}{\varepsilon_{ij}}\right)^2}$,

All the bins are included in the fit except those intersected by the Dalitz plot contour. The fit procedure has been tested on Monte Carlo and has been verified to correctly reproduce in output the input values of the parameters.
When applying the fit on the full data set we observe that the expansion up to the second order does not fit adequately the data: we find values of χ^2 probability very low, for any choice of the binning. Therefore we added to the amplitude expansion the cubic terms:

$$|A(X,Y)|^2 \simeq 1 + aY + bY^2 + cX + dX^2 + eXY + fY^3 + gX^3 + hX^2Y + lXY^2. \tag{14}$$

The values of χ^2 probability improve significantly with the inclusion of only one additional term, namely the fY^3 term; all the other cubic terms are consistent with zero and do not improve the fit quality; therefore in the following we keep only the f parameter.
Changing the bin size from $\Delta X = \Delta Y = 0.20$ to $\Delta X = \Delta Y = 0.11$, we find very similar results, showing that the fit is almost binning independent.
In table 1 are reported the fit results for $\Delta X = \Delta Y = 0.125$ (154 bins are used), where we found the best χ^2 probability, and for different parameterisations of $|A|^2$.In the first row all the parameters a, b, c, d, e, f are left free; in the following rows the C-violating c, e parameters are always set =0; in the last 3 rows we have moreover

set $d = 0$; $f = 0$ and $d = f = 0$.

dof	P_{χ^2}	$10^3\ a$	$10^3\ b$	$10^3\ c$	$10^3\ d$	$10^3\ e$	$10^3\ f$
147	73%	-1090±5	124±6	2±3	57±6	-6±7	140±10
149	74%	-1090±5	124±6		57±6		140±10
150	$< 10^{-6}$	-1069±5	104±5				130±10
150	$< 10^{-8}$	-1041±3	145±6		50±6		
151	$< 10^{-6}$	-1026±3	125±6				

Table 1

Fit results for different parameterisations of $|A|^2$. Values in 2^{nd} row are used for final results.

As expected from C-invariance in $\eta \to \pi^+\pi^-\pi^0$ decay the parameters c and e are consistent with zero, and removing them from the fit does not affect the result for remaining parameters.

We observe a quadratic slope in X and a cubic slope in Y clearly different from zero. Therefore our final results for the Dalitz plot parameters are those shown in second row of the table. Fig.5 shows a comparison between fit and data for the projections in X or Y.

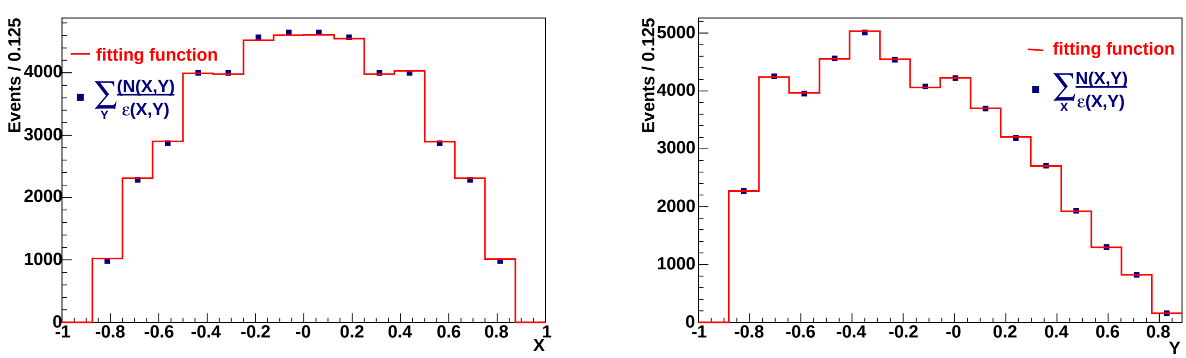

Fig. 5. Comparison between data(points) and fit(histogram) for X,Y projections of the Dalitz plot distribution.

5 Systematic uncertainties

We have estimated the systematics errors due to the following sources:

efficiency evaluation All relevant reconstruction efficiencies have been checked directly on data, using suitable control samples: the only observable systematic effect is introduced by the EVCL procedure, which we have checked with the minimum bias sample. We find a remarkable agreement between Data and MC for various kinematical distributions (see fig.6); this implies that the experimental resolution is well modelled in MC; therefore we neglect any related systematics on the signal selection efficiency $\varepsilon(X, Y)$.

resolution and binning We have checked energy resolution for the photons by comparing the distributions of the photon energies after the kinematic fit on data and MC finding good agreement for both the core and the tails of the distributions. Drift Chamber momentum resolution and absolute scale is controlled run by run by checking the K_S mass reconstructed in $K_S \to \pi^+\pi^-$ events. The effect of binning was estimated by changing the bin size by a factor of two in the range $\Delta X = \Delta Y \in [0.11, 0.20]$.

background contamination The main source of backgrounds to our analysis are:
(1) $\phi \to \eta\gamma$ with $\eta \to \pi^+\pi^-\pi^0$ and $\pi^0 \to e^+e^-\gamma$;
(2) $\phi \to \omega\pi^0$ with $\omega \to \pi^+\pi^-\pi^0$;
Although overall background contamination is small, its presence gives an observable systematic effect at our level of precision. We have changed the cut on $M_{\gamma\gamma}$ in a wide range, corresponding to B/S varying from 0.7% to 0.2% , obtaining slightly different values for the parameters.

stability with respect to data taking conditions We have divided our data sample in 9 periods of about 50 pb^{-1}each. We have verified that the results for each parameter are compatible to be constant all over the data taking and that the average values over the periods are consistent with the ones from the whole data sample fit.

radiative corrections Radiated effects have been considered by generating 10^7 $\eta \to \pi^+\pi^-\pi^0\gamma$ decays, according to ref. [16]. We have verified that the bin by bin ratio of the Dalitz plot obtained for $\eta \to \pi^+\pi^-\pi^0\gamma$ decays with the one for $\eta \to \pi^+\pi^-\pi^0$ decays can be fitted with a constant with $\chi^2/dof = 154/153$ corresponding to a χ^2 probability of 46%.

For each effect mentioned above the systematic error has been conservatively estimated as the maximum parameter variation respect to the reference one; the total systematic error is obtained by summing in quadrature the various contributions as shown in table 2.

Source	Δa	Δb	Δd	Δf
EVCL	-0.017	0.005	-0.012	0.01
binning	-0.008 +0.006	-0.006 +0.006	-0.007 +0.001	-0.02 +0.02
background	-0.001 +0.006	-0.008 +0.006	-0.007 +0.007	-0.01
Total	-0.019 +0.008	$\pm$ 0.010	-0.016 +0.007	$\pm$ 0.02

Table 2
Summary of the systematic errors on the Dalitz plot parameters.

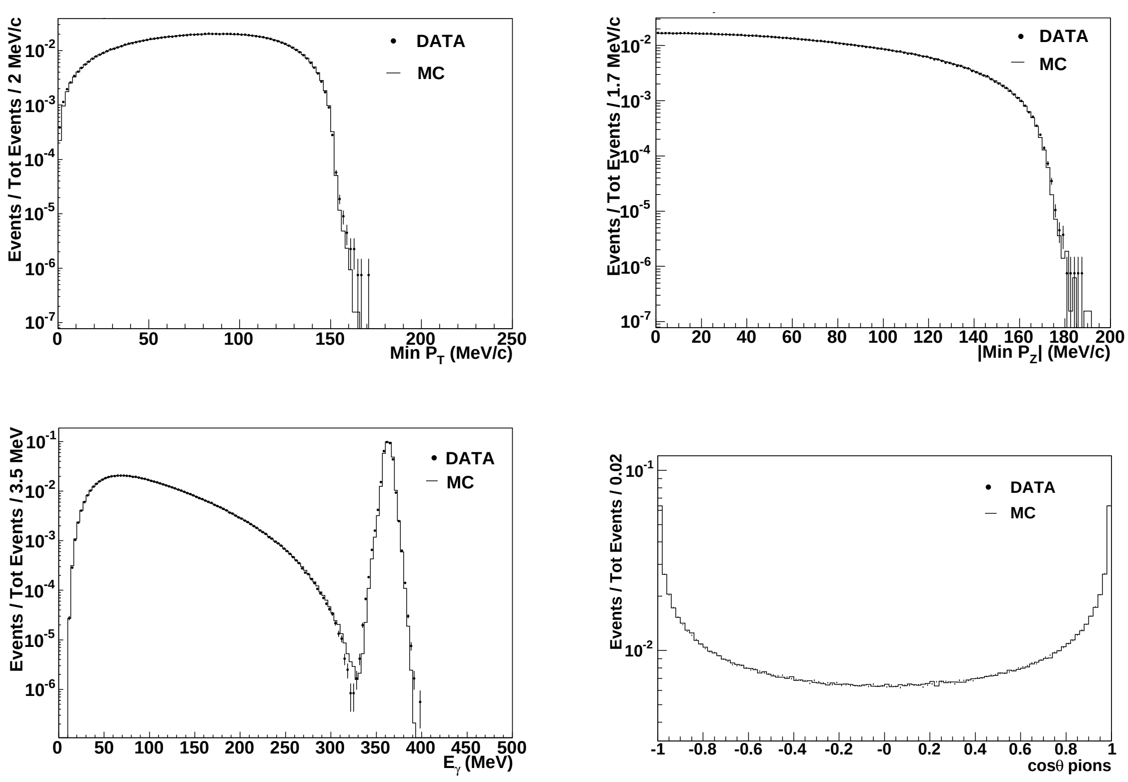

Fig. 6. Data vs MonteCarlo comparisons in log scale. From top left in clockwise direction: minimum P_T and P_Z, $\cos\theta$ between pion tracks and E_γ for photons.

6 Asymmetries

While the polynomial fit of the Dalitz plot density gives valuable information on the matrix element, some integrated asymmetries are very sensitive in assessing the possible contributions to C violation in amplitudes with fixed ΔI. In particular left-right asymmetry (which is of course strongly related to the c parameter in our fit) tests C violation with no specific ΔI constraint; quadrants asymmetry tests C violation in $\Delta I = 2$ and sextants asymmetry (for a definition see ref. [17]) tests C violation in $\Delta I = 1$.

In the following we present results on asymmetries which use 4 times the statistics entering the PDG fits. For this measurement we use the following approach: we obtain from MC the efficiency, for each region of the Dalitz plot, as the ratio between reconstructed and generated events in the region. This definition takes into account the resolution effects as well. We cross check the result by evaluating the asymmetries on Monte Carlo, these turn out to be all compatible with zero. We then evaluate the asymmetry on data by folding in the expected MC efficiency. after subtracting the MC expected background. On MC, for a sample of 5.69×10^6 events we get:

$$\varepsilon_L = (34.91 \pm 0.02)\% \qquad \varepsilon_R = (35.05 \pm 0.02)\% \qquad A_{LR} = (-0.006 \pm 0.06) \times 10^{-2}$$

$$\varepsilon_{13} = (35.01 \pm 0.02)\% \qquad \varepsilon_{24} = (34.95 \pm 0.02)\% \qquad A_Q = (-0.008 \pm 0.06) \times 10^{-2}$$

$$\varepsilon_{135} = (35.00 \pm 0.02)\% \qquad \varepsilon_{246} = (34.96 \pm 0.02)\% \qquad A_S = (-0.05 \pm 0.06) \times 10^{-2}$$

The "raw" asymmetries on data are found to be:

$$A_{LR} = (-9 \pm 9) \times 10^{-4}; A_Q = (2 \pm 9) \times 10^{-4}; A_S = (13 \pm 9) \times 10^{-4}.$$

Correcting for MC efficiencies we get:

$$A_{LR} = (9 \pm 10_{stat.}) \times 10^{-4}; A_Q = (-5 \pm 10_{stat.}) \times 10^{-4}; A_S = (8 \pm 10_{stat.}) \times 10^{-4}.$$

In assessing the systematics for the measured asymmetries we have considered all the effects taken into account for the Dalitz plot fit, namely:

- Effect of background (by varying cuts);
- Effect of EVCL (by using Minimum Bias sample);
- Data-MC efficiency comparison (using the $\phi \to \pi^+\pi^-\pi^0$ control sample)

In particular the tracking efficiency has been evaluated separately for the two charges, since in MC is evident a small but statistically significant difference in left and right efficiencies, due to a slightly different tracking efficiency as a function of p_T for positive and negative pions.

Since we require both tracks to be reconstructed the absolute value of the efficiency is not important for the asymmetry, but rather its dependence upon the pion momentum. The very good Data-MC agreement has been already demonstrated for both charges on the signal. We here use an independent control sample of $\phi \to \pi^+\pi^-\pi^0$ events and, as described before (see section 3), check the agreement between Data and MC for the efficiencies as a function of momentum the two charges. Results are shown in fig. 7. The control sample agrees well with MC within errors, and the Data-MC ratio is well fitted by a constant. In order to assess the possible systematics

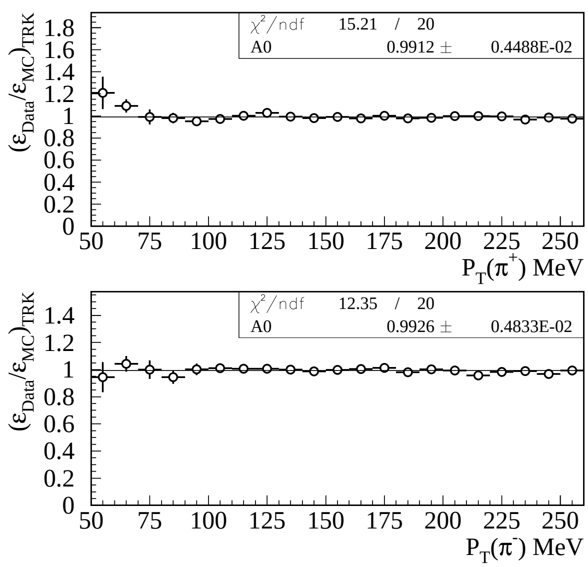

Fig. 7. The Data-MC ratio of tracking efficiency for π^+ (up) and π^- (down) as a function of the pion transverse momentum. The maximum deviation from a constant fit has been used for systematics evaluation (see text).

connected with the tracking efficiencies we have assumed a “worst case” approach: we have estimated the maximum positive or negative linear slopes compatible within one sigma with the fit of the distributions shown in fig. 7. Then we have assumed the two charges to behave with *opposite* slopes. This gives us two possibilities (π^+ with positive slope and π^- with negative slope and vice-versa). We have then reweighted the events according to these two possibilities and used the maximum difference observed in the asymmetries as an estimate of the possible systematic effects due to different Data-MC efficiencies. The systematics connected with the asymmetries are shown in table 3.

Syst. Effect	Left-Right	Quadrant	Sextant
Background	$(-0.2/+0.1)\times 10^{-3}$	$(-0.2/+0.2)\times 10^{-3}$	$(+0.3)\times 10^{-3}$
EVCL	$(-0.5)\times 10^{-3}$	$(-0.3)\times 10^{-3}$	$(+0.7)\times 10^{-3}$
Efficiency	$(-1.3/+0.9)\times 10^{-3}$	$(-0.3/+0.2)\times 10^{-3}$	$(-1.3)\times 10^{-3}$
Total	$(-1.4/+0.9)\times 10^{-3}$	$(-0.5/+0.3)\times 10^{-3}$	$(-1.3/+0.8)\times 10^{-3}$

Table 3
Systematic errors on asymmetries.

Therefore the final results for the asymmetries are:

$$A_{LR} = (0.09 \pm 0.10(\text{stat.})^{+0.09}_{-0.14}(\text{syst.})) \times 10^{-2}$$

$$A_{Q} = (-0.05 \pm 0.10(\text{stat.})^{+0.03}_{-0.05}(\text{syst.})) \times 10^{-2}$$

$$A_{S} = (0.08 \pm 0.10(\text{stat.})^{+0.08}_{-0.13}(\text{syst.})) \times 10^{-2}$$

7 Conclusions

The results including the statistical uncertainties coming from the fit and the estimate of systematics are:

$$a = -1.090 \pm 0.005(stat)^{+0.008}_{-0.019}(syst) \tag{15}$$

$$b = 0.124 \pm 0.006(stat) \pm 0.010(syst) \tag{16}$$

$$d = 0.057 \pm 0.006(stat)^{+0.007}_{-0.016}(syst) \tag{17}$$

$$f = 0.14 \pm 0.01(stat) \pm 0.02(syst) \tag{18}$$

The systematic error has been obtained adding in quadrature all the contributions in tab. 2. Tab.4 gives the correlation coefficients between the fitted parameters.

The following comments can be done:

	a	b	d	f
a	1	-0.226	-0.405	-0.795
b		1	0.358	0.261
d			1	0.113
f				1

Table 4
Error matrix from the Dalitz plot fit.

- the fitted value for the quadratic slope in Y is almost one half of the simple Current Algebra prediction ($b = a^2/4$), thus calling for significant higher order corrections;
- the quadratic term in X is unambiguously different from zero;
- similarly for the large cubic term in Y;
- when integrating the polynomial over the phase space to get the decay width, the strong correlations between parameters must be carefully taken into account for a correct error estimate.
- we don't observe any evidence for C violation in the $\eta \to \pi^+\pi^-\pi^0$ decay since the c and e parameters of the Dalitz plot and the charge asymmetries are all well consistent with zero.

References

[1] D.G. Sutherland, Phys. Lett. **23**, 384 (1996).

[2] R. Baur, J. Kambor and D. Wyler, Nucl. Phys. B**460**, 127 (1966).

[3] J. Bijnens and J. Gasser, Physica Scripta T99, 34 (2002).

[4] R. Dashen, Phys. Rev. **183**, 1245 (1969).

[5] H. Leutwyler, Phys. Lett. B**378**, 313 (1996).

[6] W. M. Yao *et al.*, J. Phys. G. **33**, 1 (2006).

[7] J. Gasser and H. Leutwyler, Ann. Phys.(NY) 150 142, (1984); Nucl. Phys. B**250 465**, (1985).

[8] B. Borasoy and R. Nissler, Eur. Phys. J. A**26**, 383, (2005).

[9] S. Guiducci *et al.*, Proc. of the 2001 Particle Accelerator Conference (Chicago, Illinois,(USA)), P. Lucas S. Webber Eds., 2001, 353.

[10] M. Adinolfi *et al.*, [KLOE Collaboration] Nucl. Instrum. Meth. A**488**, 51 (2002).

[11] M. Adinolfi *et al.*, [KLOE Collaboration] Nucl. Instrum. Meth. A**482**, 364 (2002).

[12] M. Adinolfi *et al.*, [KLOE Collaboration] Nucl. Instrum. Meth. A**492**, 134 (2002).

[13] F. Ambrosino *et al.*, [KLOE Collaboration] Nucl. Instrum. Meth A**534**, 403 (2004).

[14] C. Di Donato, KLOE Note 214, http://www.lnf.infn.it/kloe/pub/knote/kn214.ps.

[15] F. Ambrosino, T. Capussela, F. Perfetto, KLOE Note 215, Dynamics of $\eta \to \pi^+\pi^-\pi^0$, http://www.lnf.infn.it/kloe/pub/knote/kn215.ps.

[16] C. Gatti, KLOE Note 194, http://www.lnf.infn.it/kloe/pub/knote/kn194.ps.

[17] J. G. Layter *et al.*, Phys. Rev. Lett. **29**, 316 (1972).